

THE INFLUENCES OF GAS INJECTION POSITIONS ON CHARACTERISTICS OF THE VORTICITY FIELDS IN AN ELLIPTICAL STEELMAKING LADLE

Roger Pizzato Nunes, rogerpn@if.ufrgs.br

Universidade Federal do Rio Grande do Sul – Instituto de Física – Departamento de Física
Av. Bento Gonçalves 9500, Caixa Postal 15051, CEP: 91501-970 – Porto Alegre, RS, Brasil.

Julio Aníbal Morales Pereira, julio@mail.ct.ufrgs.br, **Antonio Cezar Faria Vilela**, vilela@ufrgs.br

Universidade Federal do Rio Grande do Sul – Escola de Engenharia – Departamento de Metalurgia
Av. Bento Gonçalves 9500, Setor 6, Centro de Tecnologia, Sala 222, CEP: 03306-000 – Porto Alegre, RS, Brasil.

Flávio Tadeu van der Laan, ftvdl@ufrgs.br

Universidade Federal do Rio Grande do Sul – Escola de Engenharia – Departamento de Engenharia Nuclear
Av. Osvaldo Aranha 99, 4o. andar, CEP: 90046-900 – Porto Alegre, RS, Brasil.

Abstract. *Studies on mixture in gas-stirred ladles show that the fluid flow structure inside the ladle is one of the main control parameters of the mixing process. The variation of the gas injection position determines each type of fluid flow which is obtained and has influence in a higher or in a lower degree over the mixing. In recent publications, it was showed by us that a better mixing is obtained if the number of low velocity regions in the ladle, the so called “dead zones”, is minimized. However, there are other aspects of the fluid flow structure that should be considered. The main objective of this work is to show the influences of 3 different gas-injection positions on the characteristics of the vorticity fields. For that, a physical model in reduced scale of an industrial ladle with an elliptical transversal section has been built in acrylic and has been cross-sectioned by 2 orthogonal LASER plans, named in this work as LASER Sheet A and B, for analysis with the image processing velocimetry technique. The velocity field in 2 dimensions has been measured and its associated one-dimensional vorticity field has been calculated for each one of these 3 gas-injection positions and 2 LASER Sheets. For each LASER Sheet, it has been observed 3 so different fluid flow structures in the velocity fields and, as a consequence, 3 so different vorticity fields. From analysis of the last ones, it has been verified that a more homogeneous mixing is possible related with the number of high intensity vortexes that are created and persist in the fluid flow by a time.*

Keywords: Flow visualization, secondary refining, gas-stirred ladle, and image processing velocimetry.

1. INTRODUCTION

The investigation of mixing in gas stirred ladles has received some efforts over the past years due to the industry necessity to increase its productivity by the optimization of the steelmaking process. Hence, numerous physical and mathematical modeling have been used as tools to study chemical and physical phenomena under the influence of operational variables such as ladle dimensions, ladle geometry, gas flow rate, and gas injection position, among others, during the liquid steel stirring treatment. Important works have been carried out and reported in the literature for cylindrical ladles (Mazumdar and Guthrie, 1995) but studies in elliptical ladles are still rare.

Although the cylindrical ladles are more commonly used in the worldwide metallurgical industry, it has been observed the introduction of elliptical ladles in the industrial productive process since some years ago. The elliptical ladles have been chosen without scientific investigation but because it propitiates an increasing of the volume of steel processed per each ladle. For this purpose, the investigation of the mixing inside elliptical ladles has been of our interesting during these last years.

During the secondary refine step, which is named as the metallurgy in ladle, the liquid steel is usually stirred with inert gas to remove particulate, to control temperature, to enhance reaction rates, and to eliminate composition gradients, among others. With that, it is possible to adjust the final chemical and the final thermal steel composition. Also, the injection of gas inside the ladle intensifies the refining reactions of metal/slag and propitiates that the inclusions fluctuate, forming a thin layer of slag in the bath surface. This slag is after removed in the metallurgical process.

The efficiency of these chemical and thermal processes is mainly related to the mixing phenomenon. Mixing enhances the chemical reactions and the thermal diffusion, making the steel stirred in the ladle more homogeneous. A given mixture is considered better when the analyzed fluid becomes more homogeneous in a shorter time. In the industry, a mixing time reduction assures the increase of productivity and the reduction of insumes employed in the steelmaking process (Argon gas, for example). In other words, it can be said that the mixing is directly related with the process quality.

Mixing can be understood as phenomenon that combines advection and diffusion. Considering the particular case in which the temperature is almost homogeneous inside the ladle, the thermal diffusion can be neglected. Therefore, it is

reasonable that the understanding about the fluid flow characteristics inside the ladle will provide the most important information about the mixing behavior. Several studies on mixing in gas-stirred ladles with a cylindrical shape (Mietz and Oeters, 1988) (Mietz and Oeters, 1989) (Joo and Guthrie, 1992) (Zhu *et al.*, 1995) (Becker and Oeters, 1998) have shown that the fluid flow structure inside the ladle in fact is one of the main control parameters of the mixing process. In these circumstances, complete understanding on fluid flow conditions which take place during the liquid steel stirring in the ladle is essential for optimization of the mixing process.

Different fluid flow structures can be achieved varying the operational parameters commented in the first paragraph above of this introduction, mainly the ladle geometry, the gas flow rate, and the gas injection position. The best setting and the influences of one in the other for each one of these parameters is already unknown and demands hard work on scientific research. Our current problem is relatively simplified since it has been investigated by us a metallurgical ladle that is already installed and employed in an important local industry. Therefore, the ladle geometry (an elliptical shape) has been already defined and all the productive process has been already customized for it. Any alteration in this productive process is financially impacting due to the necessity of redesigning the involved machines. In our case, it is impracticable and this alternative should be disrespected, excluding the ladle geometry as a possible operational parameter to be varied. Thereby, the gas flow rate and the gas injection position remain as the only parameters that can be changed for achieving a better mixing of the steel inside the ladle.

In this work, for simplicity, the gas flow rate will be kept constant and only the influences of the gas injection positions over the fluid flow structure will be considered. The gas injection position variation determines each type of fluid flow structure which has been obtained and has influence in a higher or lower degree over the mixing characteristics in the ladle. The influences of the gas flow rate have been currently studied by us and will be a subject of our future publications.

In recent publications (Nunes *et al.*, 2007a) (Nunes *et al.*, 2007b), it was showed by us that, also for elliptical ladles, the mixing enhancement is directly related with the number of “dead zones” that are generated in the fluid flow. By “dead zones” are understood the regions of the fluid flow in which dye tracers have difficult to arrive. However, there are other aspects of the fluid flow structure that should be considered. Much more information can be obtained calculating other relevant parameters of the fluid flow.

The main objective of this work is to show the influences of 3 different gas-injection positions, named here as PT1 (eccentric test position), PT2 (half radius test position), and PT3 (central test position) on the characteristics of the vorticity fields inside an elliptical ladle. For that, a physical model in reduced scale of an industrial ladle with elliptical transversal section has been built in acrylic and analyzed by the means of the image processing velocimetry technique. The physical model of the ladle has been cross-sectioned by 2 orthogonal LASER sheets, which are denominated here as LASER Sheet A and B. The two-dimensional velocity field has been measured for each one of these 6 configurations (2 distinct LASER Sheets and 3 distinct gas injection positions) and the vorticity field has been calculated. For each one of these gas injection positions, it has been observed 3 so different fluid flow structures and, as a consequence, 3 different vorticity fields. As a resume, it will be shown new results for 12 fields, 6 corresponding to the velocity and 6 corresponding to the vorticity.

This article is organized in the following form: in section 2, the methodology employed in the experiments is presented. In section 3, the two-dimensional velocity fields measured in the tests for each one of the above gas injection positions and LASER Sheets with its associated vorticity fields are shown. In this section, a long discussion about the obtained results is also established. In section 4, the conclusion about the analysis done in section 3 for the velocity fields and for the vorticity fields measured in the ladle physical model is presented. Finally, in section 5, it will be discussed the perspectives for future works.

2. METHODOLOGY

2.1. The developed physical model

The Figure 1 presents, without the correct aspect ratio and just for an illustrative purpose, the cross-section of the physical model of the gas-stirred ladle with an elliptical shape employed in the tests. The ladle semimajor axis has 346,5mm and its semiminor axis has 380,3mm. Its height is 820mm. The equivalence between the physical model and the industrial ladle has been obtained by geometric similarity, through a scale factor, and by dynamic similarity, derived from the equality between the Froude number of the experiment and the Froude number of the real system found in the industrial plant. How it has been previously commented in section 1, the gas flow is kept with a constant rate in the tests and has a value of 17 Nl/min, which assures compatibility with the regime operated by the industrial ladle in the plant. More information about the most important parameters of this ladle physical model and its comparison with the real ladle of the industry can be found in references (Morales *et al.*, 2006) (Nunes *et al.*, 2007a).

The physical model has been built in acrylic (its commercial name is Plexiglas), with reduced scale of 1:3, and it uses water at room temperature as a steel simulator. The bath is agitated by injection of compressed air at the ladle bottom in 3 different positions, such as PT1 (eccentric gas injection position), PT2 (half radius gas injection position), and PT3 (central gas injection position). Its locations in the ladle bottom are specified in the same Figure 1 in

millimeters. These gas injection positions have been chosen because they has been one of many already empirically used here in a local industry.

For minimization of the optical distortion on the captured frames, which are a natural consequence of the elliptical shape of the ladle, the physical model has been inserted in a transparent and rectangular reservoir filled with water.

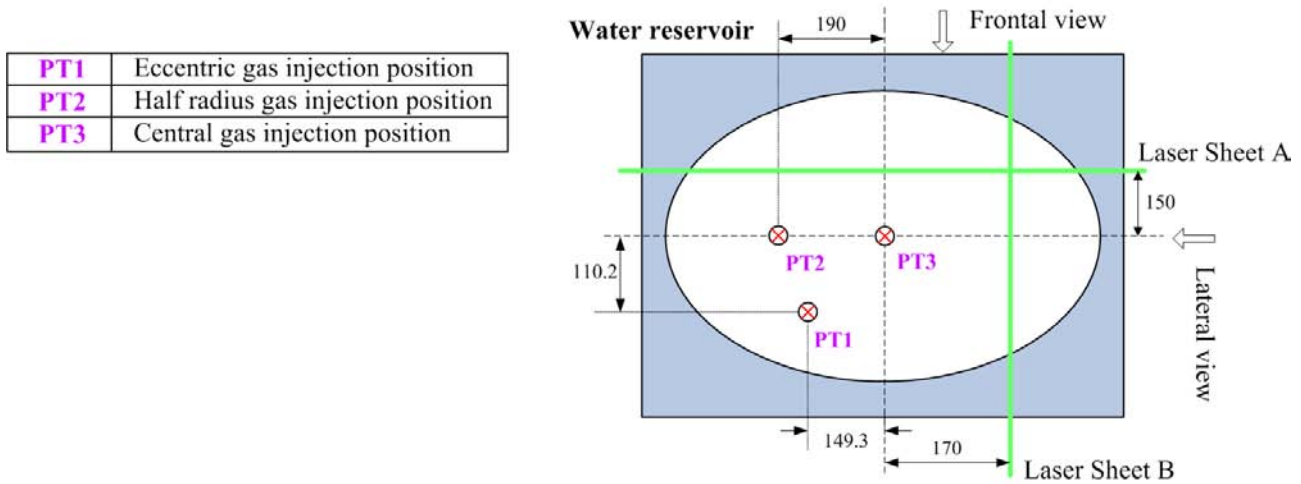


Figure 1. Transversal section of the ladle physical model employed in the tests.

2.2. Velocity field measurement technique

The Figure 2 shows the experimental equipments employed in the measurement of the velocity fields for each one of the gas injection positions and LASER Sheets exactly described in subsection 2.1. Since it has an illustrative purpose, in the Figure 2 it is shown just the LASER Sheet A. The exactly position where the physical model of ladle is cross-sectioned by the LASER Sheet B is shown in the Figure 1. This system is composed beyond the ladle by an air compressor, a pressure regulator, and a rotameter, which generate and control the gas injection that continuously excites the fluid within the ladle. The experimental system is complemented with a LASER source, optical lens, polyethylene particles, and a CCD camera.

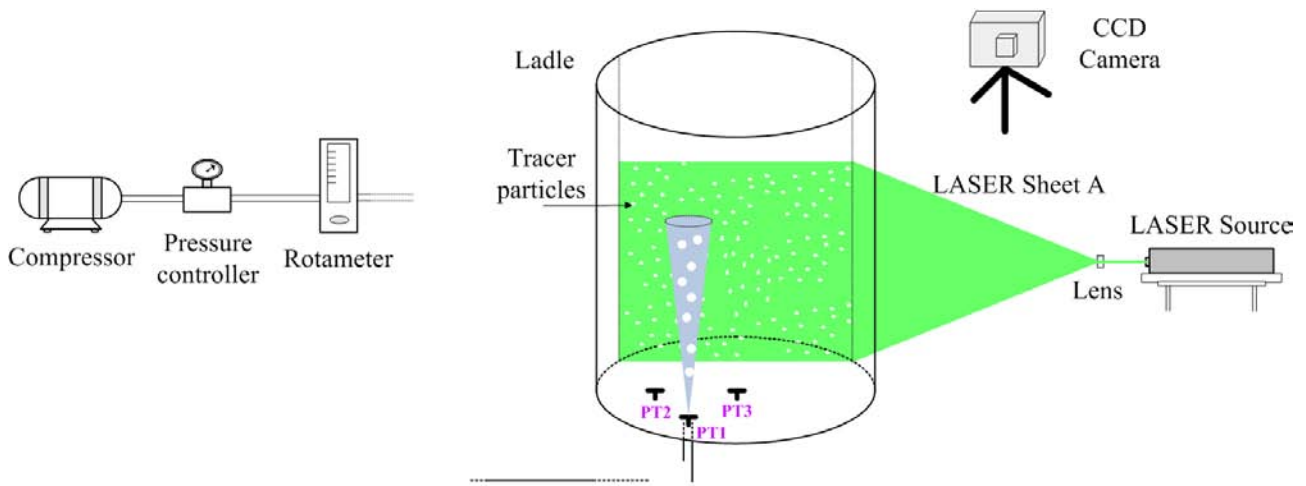


Figure 2. The ladle physical model and the instrumentation system employed in the measurements.

In order to obtain the velocity field of the fluid flow, image processing velocimetry techniques have been employed. Due to the density of polyethylene particles spread in the fluid flow, the system mode has been PIV (Particle Image Velocimetry) (Adrian, 1991). With such a technique, small tracer particles are disseminated in the fluid flow, which is irradiated by a LASER beam. This LASER beam is expanded by a cylindrical lens into a thin 2 mm vertically oriented LASER sheet. The LASER light spread by the particles is then captured by a CCD camera, which was orthogonally positioned to the flow. The CCD camera analogically stores both the space and time evolution of particles at a rate of 30Q/s. Note that, since the ladle is cross-sectioned by 2 different and orthogonal LASER Sheets A and B, the camera is also repositioned in each measurement as indicated in Figure 1 with, respectively, the Frontal view and Lateral view.

The specific position where the physical model has been cross-sectioned by each one of the LASER Sheets is presented in Figure 1.

The captured recording is digitized by a frame grabber connected to a PC, in which it is stored in AVI format. After that, the AVI video is segmented into their constituent frames, which are in the sequence stored in 8 bits grayscale Bitmap (BMP) images. Each frame represents the spatial behavior of the fluid flow in a particular instant of time. The sequence of frames provides the information about the fluid flow dynamics. From the displacement of the particles between each consecutive frame, the two-dimensional velocity vectors in the plane of the LASER sheet can be obtained through the cross-correlation mathematical operator. The velocity vectors have been computed and plotted using the IPVFlow 1.0 software, which has been developed by the authors and has less than 1% of uncertainty. Refer to (Nunes, 2005) (Nunes *et al.*, 2007a) for more details on the PIV technique.

The PIV results will be show in the section 3, where the overall analysis about the fluid flow structure inside the ladle will be done. All the measurements have been started just after some minutes that the experiment had been running. It assures that the transient behavior of the fluid flow structure disappears and only its steady behavior remains, achieving some macroscopic pseudo-equilibrium (from the point of view of the fluid flow structure). In the steady state, the fluid flow remains with the same structure. No new vortexes are created or destroyed.

All PIV results that will be presented have been averaged during 12s. This time slice is enough to catch the relevant dynamics of the fluid flow structure inside the ladle during its stirring. Note that the particular dynamical behavior of a specific spatial point of the fluid flow is unimportant here. In fact, it is important the relation between each velocity vector in each specific spatial position of the fluid flow with the other ones, which propitiates a macroscopic behavior that has influence over the fluid flow structure characteristics.

3. RESULTS AND DISCUSSION

3.1. The velocity fields

The Figure 3 to Figure 5 shows the different time-average velocity fields during a time interval of 12s for the 3 distinct gas injection positions PT1, PT2, and PT3, which are employed in the tests and are already previously described in the paragraphs of subsection 2.1, considering a fixed gas flow rate of 17NI/min. The time-average velocity fields of Figure 3a to Figure 5a correspond to the Frontal view of Figure 1, captured through the LASER Sheet A, where the time-average velocity fields of Figure 3b to Figure 5b corresponds to the Lateral view of Figure 1, captured through the LASER Sheet B. All vectors presented in these figures are in scale and has been plotted over the first frame used in the time-average process.

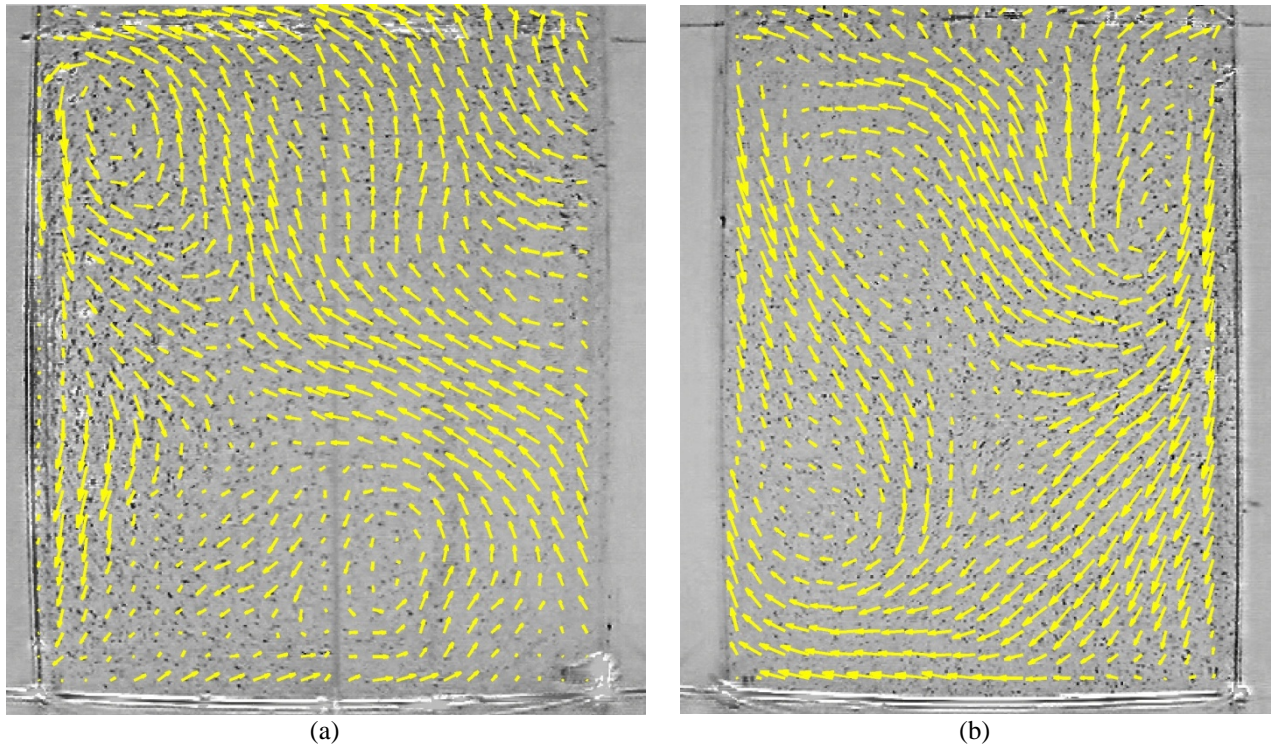


Figure 3. Average velocity field at $t=12s$ for the eccentric gas injection position PT1: (a) The frontal view (LASER sheet A), and (b) The lateral view (LASER sheet B). Gas flow rate of 17 NI/min.

For the eccentric gas injection position PT1, the velocity field from the Frontal view of Figure 3a presents a vortex on the left side, close to the ladle surface and the ladle wall, as well as another vortex centered close to the central axis of the ladle, at its bottom. The velocity field of the lateral view of this gas injection position, which is presented in the Figure 3b, shows 2 vortexes, one in the superior right corner and other in the inferior left corner. This lateral view complements the frontal view in such a way that it is possible to intuit that these views are orthogonal cross-sections of 2 three-dimensional vortexes developed inside the ladle, one in the ladle surface and other in the ladle bottom. The intensity of these vortexes, in each of its cross-sections, will be shown in the vorticity fields presented in the subsection 3.2. In accordance with the velocity field presented in Figure 3a yet, the regions belonging to both the right superior and the left inferior edge are weakly influenced by those vortexes. The result is a major amount of movement in the diagonal direction, connecting the left superior edge to the right inferior one. This is an evidence that both the right superior and the left inferior region of this ladle will take longer to be mixed with this gas injection position. In reference (Nunes *et al.*, 2007a), it has been shown by us an experiment with dye tracer that reinforce this evidence.

For the half radius position PT2, whose frontal and lateral views are shown in the Figure 4, it can be observed, both in the frontal and lateral view, a fluid flow with a great amount of small recirculation zones distributed throughout the bath. Higher velocities can be observed at the ladle bottom in relation to the eccentric gas injection position PT1 and also in relation to the central gas injection position PT3, as it will be shown by us later when analyzing its velocity fields. It is possible to count at least 4 distinct vortexes in Figure 4a. One vortex at the superior left corner of the ladle, one vortex at the ladle middle to the right and together to its lateral wall, and 2 vortexes at the ladle bottom (one in the right corner and other in the left corner). In the lateral view of the half radius gas injection position shown in Figure 4b, although it seems to be more difficult to identify, it is also possible to locate at least 3 vortexes: one vortex at the superior left corner of the ladle, one vortex at the superior right corner of the ladle, and one vortex at the ladle bottom, at its right corner together to its lateral wall.

Those small vortexes distributed over the ladle cross-sections A and B is a striking characteristic of the fluid flow structure originated through the gas injection by the position PT2. It is not a characteristic observed in the other gas injection positions, as it has been shown for PT1 and as it will be shown ahead for PT3. Also, the presence of 2 small vortexes in the ladle bottom continuously excites this region, proportionating higher velocities and an improvement of the fluid flow when compared with the others gas injection positions.

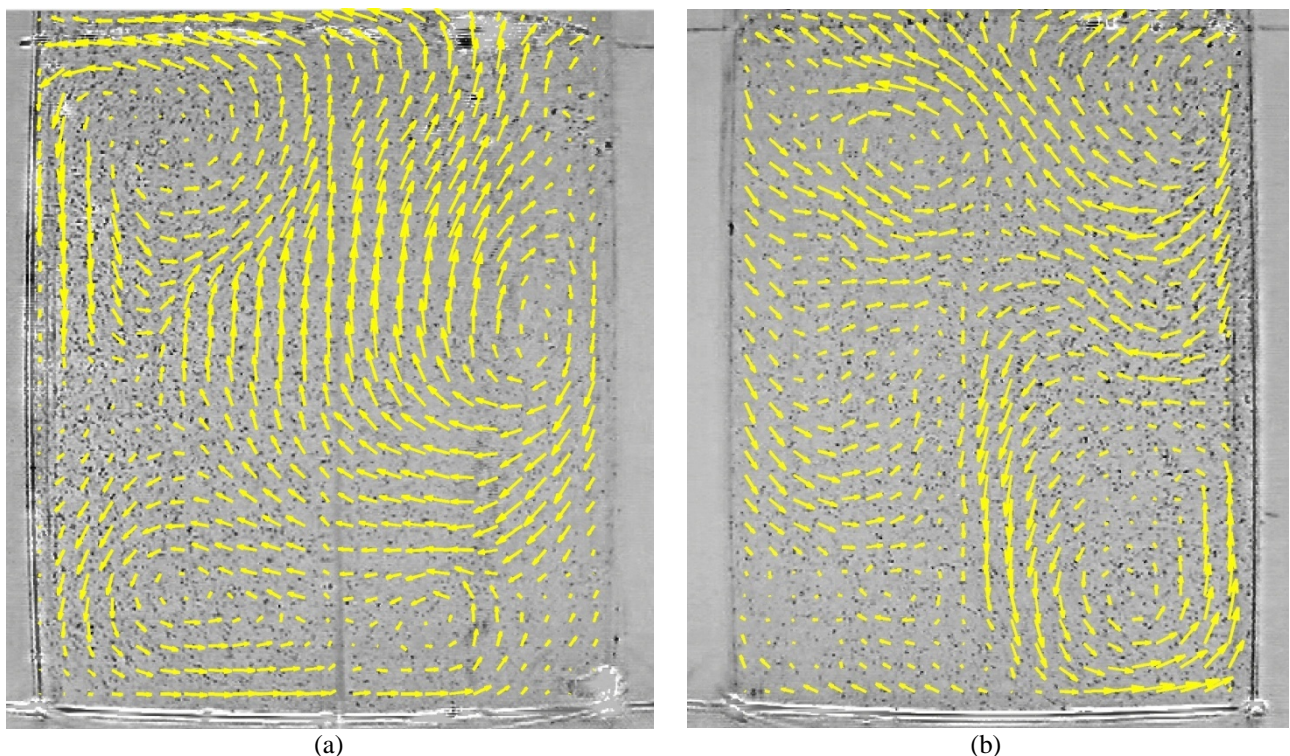


Figure 4. Average velocity field at $t=12s$ for the half radius gas injection position PT2: (a) The frontal view (LASER sheet A), and (b) The lateral view (LASER sheet B). Gas flow rate of 17 NI/min.

During the stirring with the central gas injection position PT3, it can be observed, in the frontal view of Figure 5a, 2 symmetrical vortexes close to the surface, and in both upper sides of the ladle. There is some low velocity regions at the ladle bottom, which are consistent with the behavior observed in the dye tracer experiment performed in reference

(Morales *et al.*, 2006). The 2 vortices present opposite rotation directions, originating a high rising fluid flow in the central region of the ladle that is strongly dispersed when the water-air interface is excited at the ladle surface.

In the lateral view of this central gas injection position PT3 presented in Figure 5b, it can be seen 2 vortices, one vortex close to the ladle surface, at its upper right corner, and other vortex almost in the middle of the ladle, close to the left ladle wall. The ascendant movement of the fluid flow is also visualized in this lateral view with a little bit of difference when compared with the frontal view of this same gas injection position PT3: this movement not occurs at the central axis of the ladle and it is not parallel to the last one. Also, it is possible to see a transverse flow below of the half ladle body and parallel to the ladle bottom. This information together with the previous analysis done for the frontal view of this gas injection position induce to thinking that there is a vortex with characteristic dimension that scales with the ladle base size and that is parallel to this. This vortex makes the stirring of the fluid in the ladle bottom difficult. This is a possible justification for what it is observed in fact in these velocity fields and in the dye tracer experiments that have been carried out by us. Please refer to (Nunes *et al.*, 2007a) (Morales *et al.*, 2006) for further information.

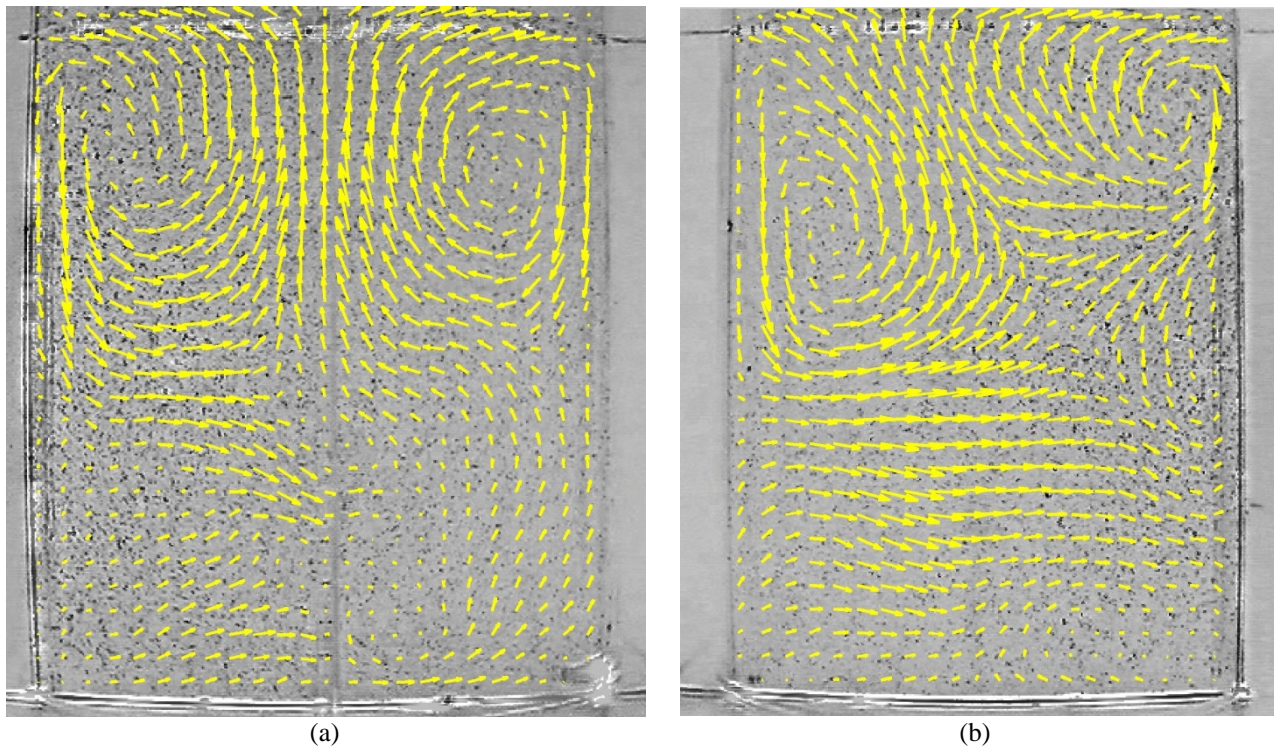


Figure 5. Average velocity field at $t=12s$ for the central gas injection position PT3: (a) The frontal view (LASER sheet A), and (b) The lateral view (LASER sheet B). Gas flow rate of 17 NI/min.

3.2. The vorticity fields

The time-average vorticity fields associated to the velocity fields presented in subsection 3.1 are shown in the Figure 7 to Figure 9 for each one of the 3 distinct gas injection positions PT1, PT2, and PT3. As in the measurement of the velocity fields, these vorticity fields have been time-averaged during a time interval of 12s, considering a fixed gas flow rate of 17NI/min. To calculate the vorticity field it has been used the central finite-difference approach. Considering that our interesting resides in the distribution of the vorticity intensity over the ladle cross-section, it has been adopted in this figures a color representation for the vorticity fields. For that, the vectorial information of the vorticity field is neglected and each absolute vorticity value has been coded with a color. More information about this representation is described in the next paragraph. Analogous to the velocity fields, the time-average vorticity fields of Figure 7a to Figure 9a corresponds to the frontal view of Figure 1, captured through the LASER Sheet A, where the time-average vorticity fields of Figure 7b to Figure 9b correspond to the lateral view of Figure 1, captured through the LASER Sheet B.

Since it is intended to do a comparative analysis between the vorticity fields calculated for each one of the gas injection positions, that is, it is desired to know which are the main differences between the vorticity fields obtained with each one of the gas injection positions and for each LASER Sheet, it has been decided to normalize all vorticity fields. To that end, for each LASER Sheet, it has been looked for the highest vorticity value of ω_{max} found in all gas injection positions. Then, the entire vorticity field for all the gas injection positions used in the tests has been divided by this highest value of ω_{max} .

In Table 1 it is presented all the highest values found in each gas injection position and for each one of the LASER Sheets A and B. The information about the LASER Sheet is shown between parentheses, after the specification of each gas injection position. From this table, it can be seen that the highest value of ω_{\max} for the LASER Sheet A is 1.813s^{-1} and occurs for the gas injection position PT3, and the highest value of ω_{\max} for the LASER Sheet B is 2.619s^{-1} and occurs also for the gas injection position PT3. These values have been stamped with blue in this table. Also, for the LASER Sheet A, it can be seen that the values for the maximum vorticity ω_{\max} are lower than $\sim 1.8\text{s}^{-1}$ for all gas injection positions, with a difference between the lower and the higher of $\sim 1.0\text{s}^{-1}$. Nevertheless, this not occurs for LASER Sheet B, where the difference between these values approaches $\sim 1.62\text{s}^{-1}$.

Table 1. Maximum values present in the vorticity fields for each one of the gas injection positions and LASER Sheets.

Gas injection position	PT1 (A)	PT2 (A)	PT3 (A)	PT1 (B)	PT2 (B)	PT3 (B)
ω_{\max} (s^{-1})	0.881	1.473	1.813	0.998	1.308	2.619

The color bar used to code each vorticity value is shown in Figure 6. To have an idea about the dimensional value of the vorticity field in a specific spatial position of the figures shown below, it is just necessary to verify its color in the vorticity field, to look for its associated dimensionless value in the color bar of Figure 6, and to multiply this value by ω_{\max} , taking care of from which LASER Sheet this value corresponds. It will be established as a threshold in our analysis the green regions of the ladle, in which the time-average absolute value vorticity is about 50% of ω_{\max} .

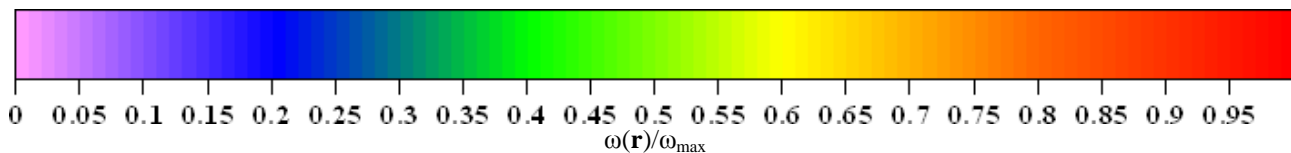


Figure 6. Color bar used in the vorticity graphics.

In the frontal view of the eccentric gas injection position PT1 presented in Figure 7a, it can be observed 3 ladle regions where the vorticity intensity has relevant values. One region is at the left upper corner of the ladle, one region is at the ladle bottom close to its central axis, and the last one region is almost at the middle of the ladle body, in the left, together to its wall. The first and the second regions commented above corresponds to the 2 vortices described when the velocity field of this gas injection position has been analyzed in the subsection 3.1. The third and last is a small region whose vorticity characteristic does not explicitly appear in the velocity field, but also stands out in the vorticity field when compared with the remainder regions of the ladle. The maximum value of vorticity observed in Table 1 occurs in the first region described above, which appears in red in the Figure 7a.

Considering Figure 7b, the lateral view of the ladle when it is stirred with the eccentric gas injection position PT1, it can be seen 2 regions in the upper half of the ladle body, one region at the left ladle corner and the other one at the right ladle corner. The right region coincides with the vortex shown in the velocity field of Figure 3b and is the region with the more intense vorticity values that appears in this field. The left region contains vorticity values a little bit smaller than the left region and which is not directly related with a spatially localized vortex, as it has been shown in its velocity field of Figure 3b. It is also possible to observe in this Figure 7b that the vortex localized at the inferior left corner of the ladle, which is spatially well-defined in the velocity field of Figure 3b, is much less intense than the right superior one, reason by which it appears almost blue in the Figure 7b.

For the half radius gas injection position PT2, the vorticity fields for its frontal and its lateral views are shown respectively in the Figure 8a, and in the Figure 8b. For both frontal and lateral view it is possible to see better here the main characteristic observed in its velocity fields of Figure 4: there are a lot of regions of the ladle disseminated over its currently analyzed cross-section where the vorticity assumes high values. For the frontal view of PT2, it is possible to count at least 4 distinct ladle regions in which the vorticity has high values. One region is localized at the superior left corner of the ladle, one region at the ladle middle to the right and together its lateral wall, and 2 regions at the ladle bottom, one in the left side of the ladle axis and other in the right side of the ladle axis. These ladle regions coincides with the regions where the vortices have been previously mapped in the velocity field of Figure 4. Still in this figure, it can be viewed some other small ladle regions where the vorticity field assumes important values.

Considering now the lateral view of the half radius gas injection position PT2, shown in Figure 4b, it is possible to observe at least 4 ladle regions with vorticity values higher than the previously established threshold. One region is located at the superior left corner of the ladle, one region is located at the superior right corner of the ladle, and the last one region at the ladle bottom, at its right corner together to its lateral wall, and extending itself until the ladle axis. As commented in the subsection 3.1, this distribution of vorticity zones with high intensity values over the ladle cross-section is a strong characteristic of the gas injection position PT2, which is not observed in the other gas injection positions PT1 and PT3. It is supposed by us that this is the reason by which the gas injection position PT2 presents a

smaller mixing time, and then a better mixing, in the dye tracer tests that have already been performed by us and that is described in the references (Morales *et al.*, 2006) (Nunes *et al.*, 2007a).

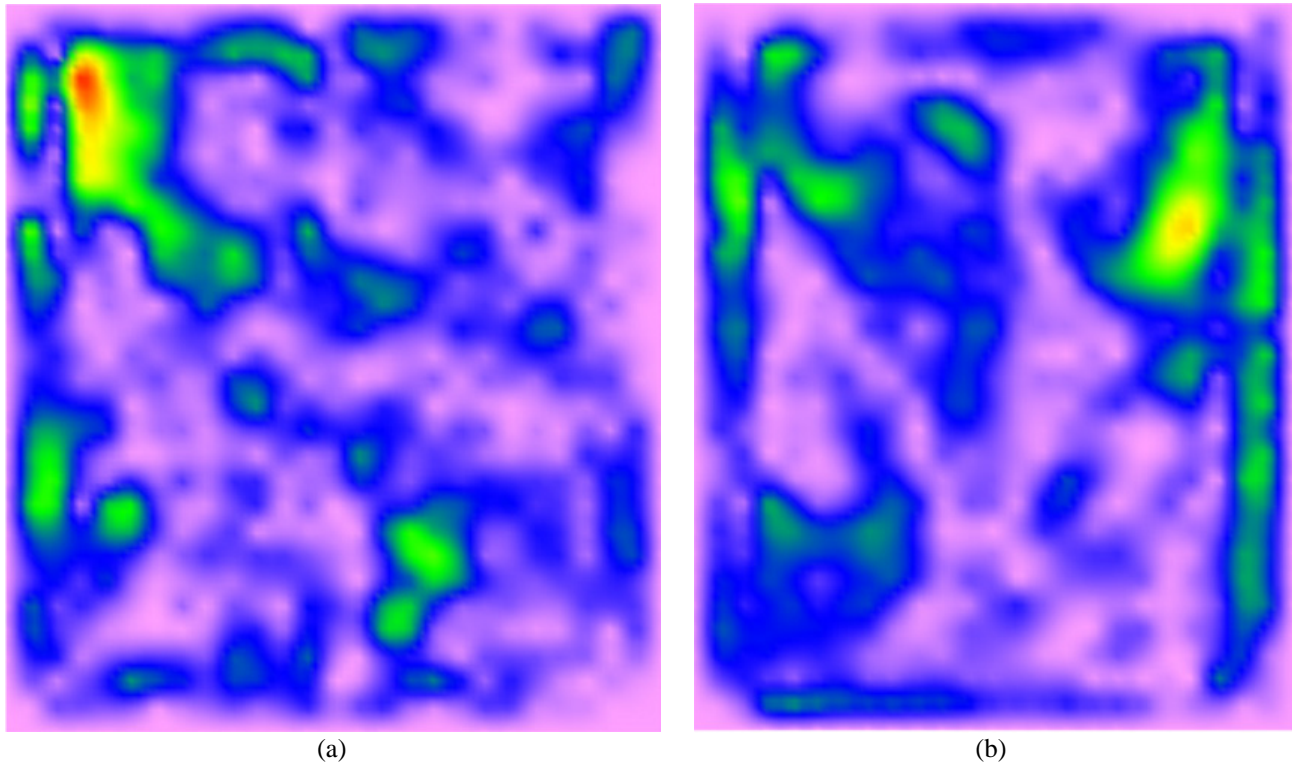


Figure 7. Average vorticity field at $t=12s$ for the eccentric gas injection position PT1: (a) The frontal view (LASER sheet A), and (b) The lateral view (LASER sheet B). Gas flow rate of 17 NI/min.

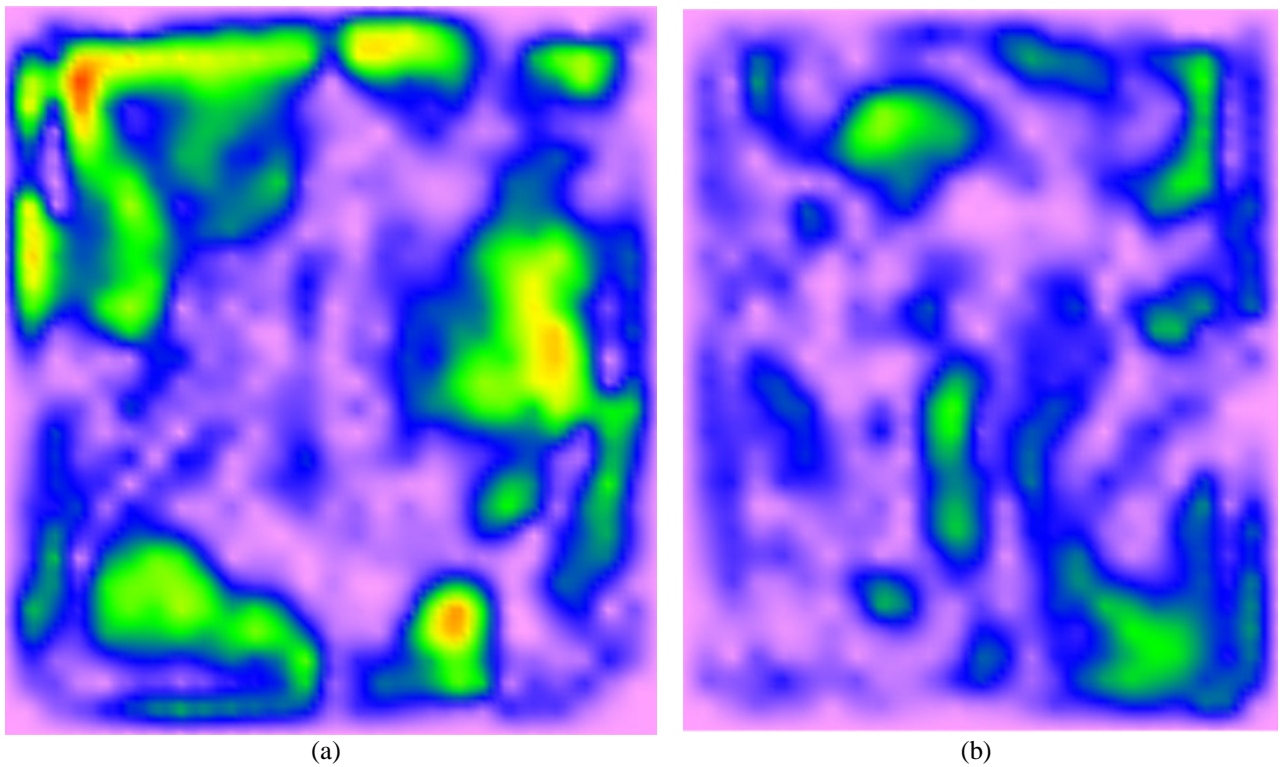


Figure 8. Average vorticity field at $t=12s$ for the half radius gas injection position PT2: (a) The frontal view (LASER sheet A), and (b) The lateral view (LASER sheet B). Gas flow rate of 17 NI/min.

Finally, in the Figure 9, it is presented the vorticity fields for the central gas injection position PT3. In the frontal view of Figure 9b, it can be noted 2 large ladle regions in which the vorticity has high values. One of these regions is found at the right superior corner of the ladle, and the other one is observed at the left superior corner of the ladle. This evidences that the 2 vortices that has been already observed in the velocity fields of Figure 5a are in fact high intensity vortices that strongly affect the flow in this superior half of the ladle body. Despite of the velocity field in the inferior half of the ladle body of Figure 5a presents small velocities, in the Figure 9a it can be seen small zones of considerable vorticity intensity, close to the ladle axis. This should be due to the ascendant movement of the gas injected in the ladle base, which excites the fluid in this zone but not excites the fluid in the inferior corners of the ladle. However, the same characteristic observed when analyzing the velocity fields remains: for the central gas injection position PT3 the absolute values of the velocity field as the absolute values of the vorticity field are more intense in the superior half of the ladle body than its observed values in the inferior half of the ladle body.

In the lateral view of the central gas injection position PT3 presented in Figure 9b, it is seen 2 ladle regions where the vorticity field assumes expressive values. One region is close to the ladle surface, at its upper right corner, and the other one is almost in the middle of the ladle, close to its left wall. These regions surround the ascendant movement of the fluid that has been visualized in this same lateral view in the previous analysis done in subsection 3.1 to the velocity field of Figure 5b. A simple overview over the lateral view shown in Figure 9b makes clear that for the gas injection position PT3 the high values of vorticity lies on the superior half of the ladle body. In the inferior half of the ladle body, the vorticity values is very small, emphasizing what is observed in the velocity field of Figure 5b. In this region, the flow has a well-defined behavior, coming from the left side to the right side of the ladle, parallel to the ladle base. This is other evidence for our initial assumption that there is a vortex with characteristic dimension that scales with the ladle base size and that is parallel to this, making the stirring of the fluid with this gas injection position PT3 difficult in the ladle bottom.

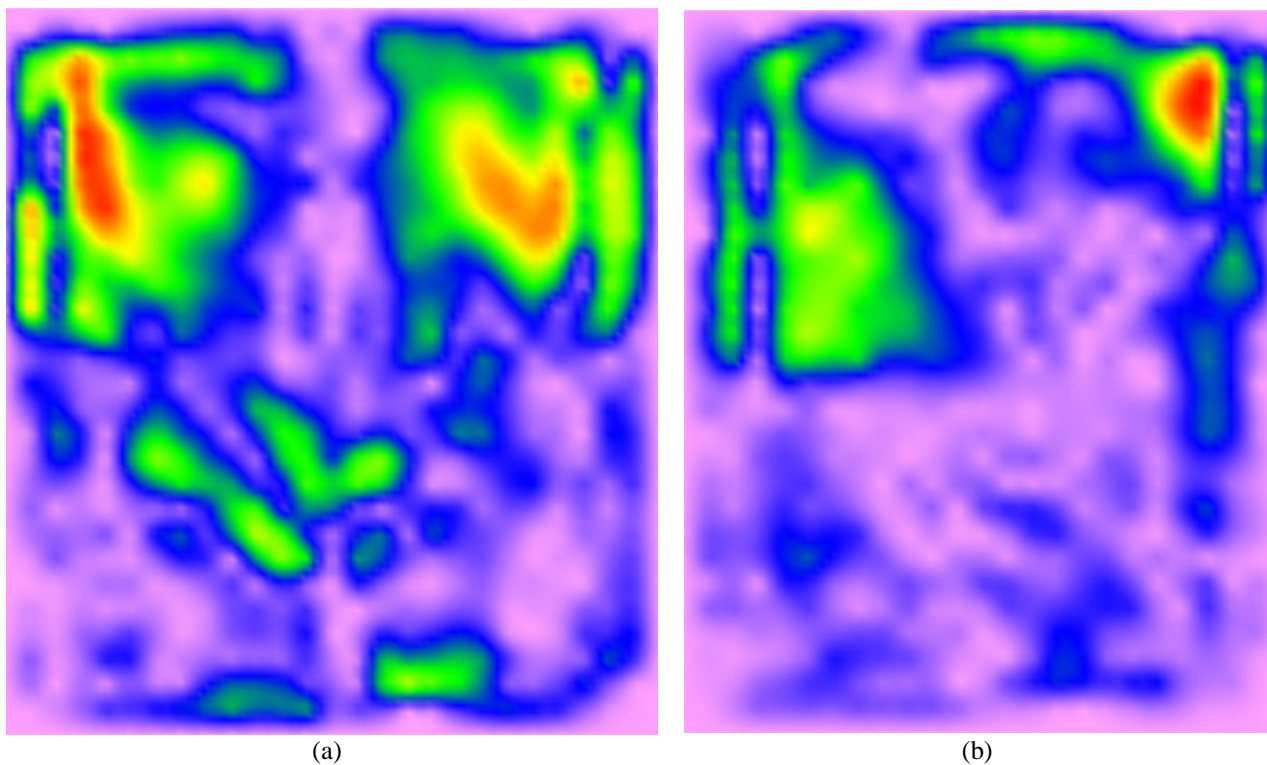


Figure 9. Average vorticity field at $t=12s$ for the central gas injection position PT3: (a) The frontal view (LASER sheet A), and (b) The lateral view (LASER sheet B). Gas flow rate of 17 NI/min.

4. CONCLUSIONS

In this work it has been presented a qualitative analysis to the one-dimensional vorticity fields obtained by the Image Processing velocimetry technique in a metallurgical ladle for 3 different gas injection positions. For that, a physical model in reduced scale of an industrial ladle with elliptical transversal section has been built in acrylic and analyzed by the means of the PIV technique for the measurement of its velocity fields. The gas injection positions used here has been the PT1 (eccentric test position), PT2 (half radius test position), and PT3 (central test position) and the gas flow rate has been kept constant to 17NI/min in the experiments. The ladle physical model has been cross-sectioned by 2 orthogonal LASER sheets, named as LASER Sheet A and B. For each one of these gas injection positions and each one

of LASER Sheets, the velocity field and its vorticity field have been measured, totalizing 12 fields to be analyzed. These results are new in the literature and shows to be substantively important for the understanding of previously experiments carried out by us through dye tracers. All of these ones are important elements to investigate the mixing phenomenon inside the ladle.

The qualitative analysis of the velocity field together with its associated vorticity field propitiated to investigate each type of fluid flow structure that is obtained with each one of the gas injection positions used here. The qualitative analysis shows to be important and is a starting point for the planning of future quantitative analysis.

The analyzed velocity fields together with its vorticity fields show 3 so different fluid flow structures. The fluid flow obtained with the gas injection position PT1 has been mainly characterized by two high intensity vortexes, one in the frontal view, at the superior left corner of the ladle, and one in the lateral view, at the superior right corner of the ladle. To the point of view of the vorticity intensity, this gas injection position presents few regions with high values.

For the gas injection position PT2, it is observed a large quantity of considerable small zones with high intensity vorticity disseminated over the ladle cross-sections. We believe that this distribution of small vortexes with high intensity in the fluid flow is a key factor for obtaining better mixings inside the ladle. This is in accordance with some of our previous results using dye tracer (Morales *et al.*, 2006), in which the gas injection position PT2 presented the lowest mixing time, and with our previous analysis of the ladle activation (Nunes *et al.*, 2007b). But this is only an indicative, we must do some other calculations to assure that.

Finally, the gas injection through PT3 generates a fluid flow structure with 2 high intensity vortexes at the superior half of the ladle body. These vortexes continuously excites this ladle region, ejecting fluid upward and originating dissipation of its energy when it reaches the water-air interface at the ladle surface. The inferior half of the ladle body remains almost unchanged for this gas injection position.

5. FUTURE WORKS

In future works, it will be presented by us the results for the Reynolds Stress, which has been just calculated and shows important information about the fluid flow inside the ladle. This new measured quantity will complement our current analysis, allowing us to understand more about which gas injection position propitiates the better mixing. Also, the results for the velocity field and the vorticity field showed here will be used to estimate quantitatively its distribution over the ladle.

6. REFERENCES

- Adrian, R.J., 1991, "Annual Reviews in Fluid Mechanics", vol. 23, pp. 261-304.
- Becker, J., and Oeters, F., 1998, "Model experiments of mixing in steel ladles with continuous addition of the substance to be mixed", *Steel Research*, 69, no. 1, pp. 8-16.
- Joo, S., and Guthrie, R.I.L., 1992, "Modeling Flows and Mixing in Steelmaking Ladles Designed for Single- and Dual-Plug Bubbling Operations", *Metallurgical Materials Transactions B*, 23B, pp.765-778.
- Mazumdar, D., and Guthrie, R.I.L., 1995, "The Physical and Mathematical Modeling of Gas Stirred Ladle Systems", *ISIJ International*, vol. 35, no. 1, pp.1-20.
- Mietz, J., and Oeters, F., 1988, "Model Experiments on Mixing Phenomena in Gas-Stirred Melts", *Steel Research*, 59, no. 2, pp. 52-59.
- Mietz, J., and Oeters, F., 1989, "Flow field and mixing with eccentric gas stirring", *Steel Research*, 60, no. 9, pp. 387-394.
- Morales, J.A., François, M.G., Ribeiro, J.L.D., and Vilela, A.C.F., 2006, "Variation on the geometric profile of a steelmaking ladle and its effect on the mixing", *Steel Grips* 4, no.1, pp. 34-42.
- Nunes, R.P., 2005, "Projeto e Implementação de um Sistema de Instrumentação Eletro-Eletrônica para Caracterização de Escoamentos através de Processamento Digital de Imagens", *Dissertação de Mestrado*, Universidade Federal do Rio Grande do Sul, Escola de Engenharia, Porto Alegre.
- Nunes, R.P., Morales, J.A., Vilela, A.C.F., and van der Laan, F.T., 2007a, "Visualization and analysis of the fluid flow structure inside an elliptical steelmaking ladle through image processing techniques", *Journal of Engineering Science and Technology*, vol. 2, no. 2, pp. 139-150.
- Nunes, R.P., Morales, J.A., Vilela, A.C.F., and van der Laan, F.T., 2007b, "Characterization of the Dead Zones in a Physical Model of a Steelmaking Ladle Through Particle Image Velocimetry", *IEEE Transactions on Instrumentation and Measurement*, submitted.
- Zhu, M.Y., Inomoto, T., Sawada, I., and Hsiao, T.C., 1995, "Fluid Flow and Mixing Phenomena in the Ladle Stirred by Argon Through Multi-Tuyere", *ISIJ International*, vol. 35, no. 5, pp. 472-479.

7. RESPONSIBILITY NOTICE

The authors are the only responsible for the printed material included in this paper.